UC Office of the President
Recent Work

Title

Evaluation of tumor ischemia in response to an indole-based vascular disrupting agent using BLI and (19)F MRI.

Permalink

Journal

ISSN

Authors

Zhou, Heling
Hallac, Rami R
Lopez, Ramona
et al.

Publication Date

2015

Peer reviewed

Original Article
Evaluation of tumor ischemia in response to an indole-based vascular disrupting agent using BLI and ^{19}F MRI

Heling Zhou[1], Rami R Hallac[2], Ramona Lopez[1], Rebecca Denney[1], Matthew T MacDonough[4], Li Li[1], Li Liu[1], Edward E Graves[3], Mary Lynn Trawick[4], Kevin G Pinney[4], Ralph P Mason[1]

[1]Department of Radiology, University of Texas Southwestern Medical Center, Dallas, TX 75390, USA; [2]Analytical Imaging and Modeling Center, Children's Medical Center, Dallas, TX 75235, USA; [3]Department of Radiation Oncology and Radiology, Stanford University, CA, USA; [4]Department of Chemistry and Biochemistry, Baylor University, Waco, TX 76798, USA

Abstract: Vascular disrupting agents (VDAs) have been proposed as an effective broad spectrum approach to cancer therapy, by inducing ischemia leading to hypoxia and cell death. A novel VDA (OXi8007) was recently reported to show rapid acute selective shutdown of tumor vasculature based on color-Doppler ultrasound. We have now expanded investigations to noninvasively assess perfusion and hypoxiation of orthotopic human MDA-MB-231/luc breast tumor xenografts following the administration of OXi8007 based on dynamic bioluminescence imaging (BLI) and magnetic resonance imaging (MRI). BLI showed significantly lower signal four hours after the administration of OXi8007, which was very similar to the response to combretastatin A-4P (CA4P), but the effect lasted considerably longer, with the BLI signal remaining depressed at 72 hrs. Meanwhile, control tumors exhibited minimal change. Oximetry used ^{19}F MRI of the reporter molecule hexafluorobenzene and *FREDOM* (Fluorocarbon Relaxometry using Echo Planar Imaging for Dynamic Oxygen Mapping) to assess pO_2 distributions during air and oxygen breathing. pO_2 decreased significantly upon the administration of OXi8007 during oxygen breathing (from 122 ± 64 to 34 ± 20 Torr), with further decrease upon switching the gas to air (pO_2 = 17 ± 9 Torr). pO_2 maps indicated intra-tumor heterogeneity in response to OXi8007, though ultimately all tumor regions became hypoxic. Both BLI and FREDOM showed the efficacy of OXi8007. The pO_2 changes measured by *FREDOM* may be crucial for future study of combined therapy.

Keywords: Vascular disrupting agents (VDAs), bioluminescence imaging (BLI), oximetry, hypoxia, ^{19}F MRI, hexafluorobenzene, OXi8007, CA4P

Introduction

Vascular disrupting agents (VDAs), a new class of anti-cancer drugs, selectively damage the endothelial cells of tumor blood vessels, inducing hypoxia and necrosis of tumor cells [1-3]. They have attracted attention because vascular endothelial cells are readily accessible through the circulatory system [4], they are less likely to develop genetic mutations leading to drug resistance [5], and the damage to tumor cells should be amplified from the blood vessel to all downstream cells depending on the oxygen and nutrition supply [6].

Many vascular disrupting agents target and bind tubulin, which is an important component of the cytoskeleton [1, 7]. Microtubules are crucial in maintaining cell morphology and a number of important cellular processes, such as intracellular transport and mitosis. Tubulin-binding VDAs destabilize microtubules leading to endothelial cell retraction, rounding and detachment, causing blood vessel leakage and increased resistance to blood flow [7, 8]. Loss of vessel wall rigidity may lead to vasoconstriction and blood vessel collapse due to the high interstitial fluid pressure. Platelet activation and clotting cause further decrease of flow [7]. The tumor specificity of VDAs may be attributed to the immaturity of tumor vasculature, especially lack of pericytes and incomplete basement membrane and endothelial cell lining [9].
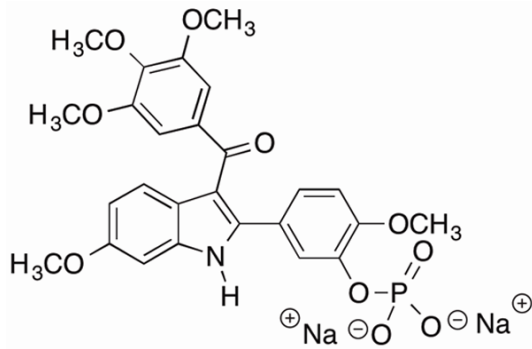
Figure 1. Molecular structure of OXi8007.

OXi8007 (**Figure 1**) is a water soluble phosphate prodrug of OXi8006, a newly developed indole-based VDA inspired by combretastatin A-4 phosphate (CA4P) and colchicine [10-13]. Recent work (manuscript in preparation) has shown potent microtubule disrupting activity caused by extensive reorganization of the cytoskeletal network in rapidly proliferating human umbilical vein endothelial cells (HUVECs). In a separate study, color Doppler ultrasound revealed rapid acute selective shutdown of vasculature in a PC3 human tumor xenograft growing orthotopically in a SCID mouse, while normal surrounding tissue was spared [12]. Bioluminescence imaging (BLI) is a noninvasive technique based on the expression of luciferase enzyme, and the presence of the substrate luciferin, oxygen and ATP. It is widely used to monitor tumor growth [14]. Recently dynamic studies have been used to assess vascular impairment caused by VDAs [1, 15], based on the reduced delivery of substrate luciferin and consequent diminished light emissions. Dynamic BLI is attractive as a sensitive, cost effective high throughput imaging technique and has been validated against dynamic contrast MRI, power Doppler ultrasound and histology [15-17].

The rapid shut down of tumor vasculature is expected to cause tumor hypoxia [1, 18-21], a vital parameter, if the drug were to be used in combination with radiotherapy [21, 22]. While many diverse invasive and non-invasive techniques may be used to assess tumor oxygenation [23, 24], here we have used a quantitative ^{19}F MRI method. *FREDOM* (Fluorocarbon Relaxometry using Echo Planar Imaging for Dynamic Oxygen Mapping) is a ^{19}F based oximetry technique that provides quantitative dynamic maps of the partial pressure of oxygen (pO_2) based on the spin-lattice relaxation of the reporter molecule hexafluorobenzene (HFB) [25].

In this study, we have applied dynamic bioluminescence imaging to assess the time course of changes in the overall tumor perfusion induced by OXi8007 up to 72 hours in an orthotopic breast cancer mouse model. Consequent acute hypoxiation has been measured using *FREDOM* MRI.

Materials and methods

Cell preparation

MDA-MB-231/luc (231/luc) cells (original source ATCC, immediate source from Dr. Graves), a human breast cancer cell line, were stably transfected to express luciferase via lentivirus as described previously [26]. Cells were incubated in Dulbecco's modified Eagle's medium (DMEM) with 10% FBS, 1% *L*-glutamine and 1% penicillin-streptomycin at 37°C with 5% CO_2. Once 80% confluence was reached, the cells were harvested, and suspended in serum-free medium.

Animals

All animal procedures were approved by the Institutional Animal Care and Use Committee of the University of Texas Southwestern Medical Center. Female SCID mice (n = 14 for BLI and n = 6 for MRI; 10-12 weeks old; weighing 20-25 g; obtained from the UT Southwestern breeding colony) were anesthetized with inhalation of 2% isoflurane. 231/luc cells (1 × 10^6 in 100 μl of PBS and Matrigel® solution, 1:1) were injected directly into the left upper mammary fat pad and tumors were allowed to grow to about 5-8 mm in diameter prior to imaging.

Bioluminescence imaging

BLI was performed using an IVIS® Spectrum system (Perkin-Elmer (Xenogen), Alameda, CA). Anesthesia was induced in an induction chamber (breathing O$_2$ plus isoflurane (Henry Schein, Inc., Melville, NY) and maintained with isoflurane (2%) in oxygen (1 dm³/min). *D*-luciferin (128 mg/kg in PBS in a total volume of 80 μl; Gold Biotechnology Inc., St. Louis, MO) was
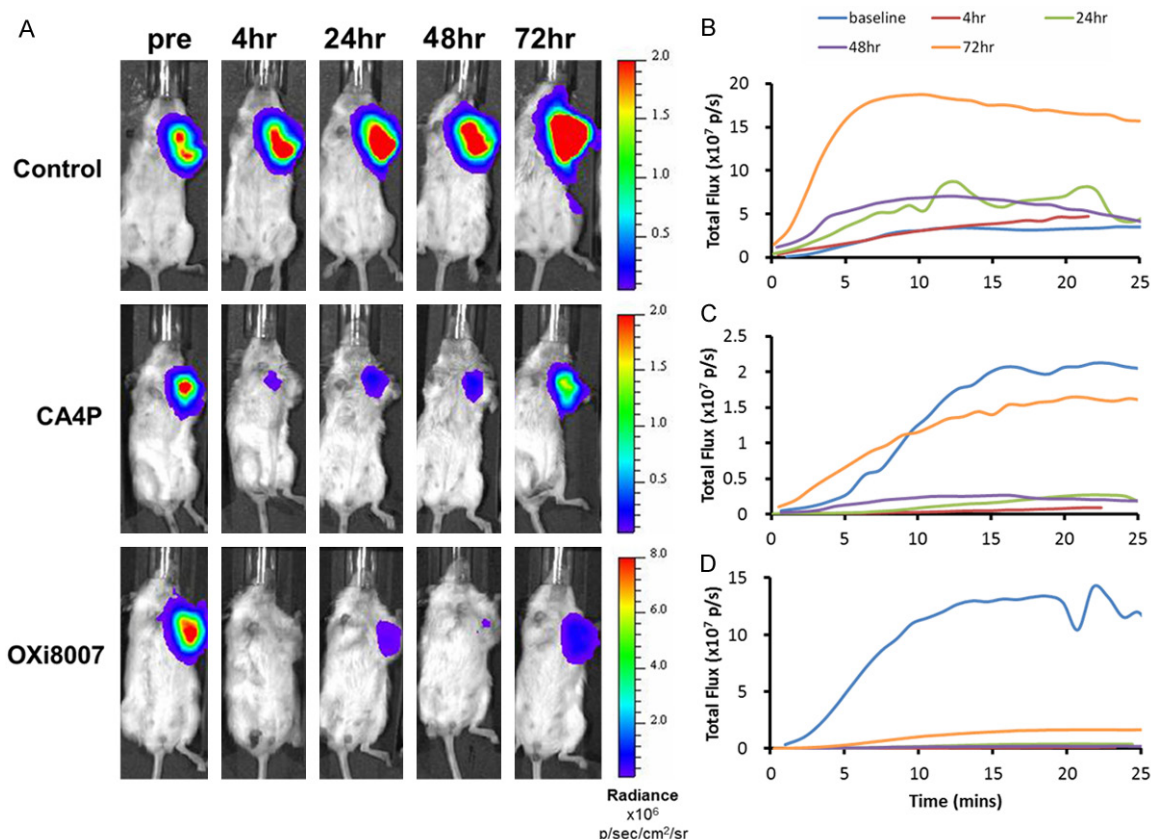
Figure 2. BLI monitoring of 231/luc orthotopic breast tumor response to IP administration of saline, CA4P or OXi8007. A. Maximum BLI signal was observed around 15 minutes post SC injection of luciferin at baseline, 4, 24, 48 and 72 hours post injection of saline (control), CA4P and OXi8007 in representative mice. B-D. Corresponding dynamic time courses of total flux obtained at the five time points for these three mice (B. Saline; C. CA4P; D. OXi8007).

administered subcutaneously (SC) in the fore-back neck region. Immediately after luciferin injection, a series of BLI images was acquired over a period of 25 minutes using auto exposure time (ranging from 1 to 60 s depending on the intensity; f-stop = 1, stage setting = D, binning = 16). Following baseline BLI, mice were treated intraperitoneally (IP) with VDA dissolved in saline. Six mice received OXi8007 (350 mg/kg; synthesized by the Pinney Research Group, as reported [12]), four received CA4P (120 mg/kg; OXiGENE Inc., South San Francisco, CA) and four received saline vehicle as control. Dynamic BLI was repeated 4, 24, 48 and 72 hours post-treatment.

Data were quantified with the Living Imaging© software as total flux (photons/s) in a region-of-interest (ROI), manually drawn to outline the BLI signal of each tumor region and automatically applied to serial images. Maximum radiance and area under the curve (AUC) for the first twenty minutes were calculated from each

dynamic curve. Data are presented as mean ± standard error (SE).

MRI

MRI used a horizontal bore 4.7-T magnet (Varian, Palo Alto, CA) with homebuilt 2 or 3.5 cm single-turn solenoid coils, tunable to ^{1}H or ^{19}F. Animals were anesthetized with isoflurane (1.5%) in air (1 L/min) and kept warm using a circulating warm water blanket. Animal body temperature and respiration were monitored with a small animal physiological monitoring system (Small Animal Instruments, Inc. Stony Brook, NY) throughout the experiment.

Quantitative pO_2 measurements were achieved using the *FREDOM* approach. Briefly, hexafluorobenzene (HFB, 50-100 µl, Lancaster, Gainesville, FL) was injected directly into the tumor with a custom-made fine sharp needle (32G; Hamilton syringe, Reno, NV). Injection was performed in a fan shape in a single plane,
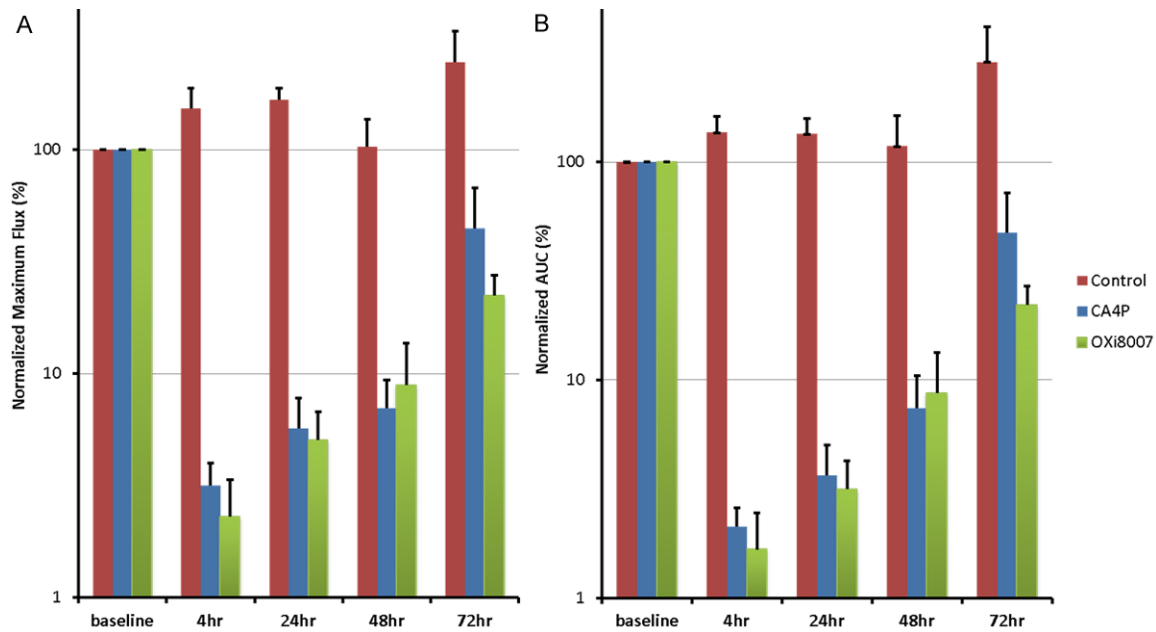
Figure 3. Summary of BLI results for the treatment groups. (A) Relative maximum light flux and (B) integrated area under the light emission curve following treatment: saline (control, n = 4), CA4P (120 mg/kg; n = 4) and OXi8007 (350 mg/kg; n = 6). Error bars represent standard error.

as recommended [25], to ensure distribution of HFB. Pulse burst saturation recovery (PBSR) echo planar imaging (EPI) was used to measure the spin-lattice relaxation rate, R_1, of HFB by arraying 14 delay times (Tau). The *FREDOM* parameters were: TR = 50 ms, TE = 21 ms, Tau range = 0.2 to 90 s, NEX = 1 to 12 (depending on Tau), FOV = 40 × 40 mm with 32 × 32 acquisition matrix, slice thickness 10 mm, giving a total acquisition time of 6½ minutes. As a baseline, three pO_2 measurements were obtained breathing air, and four with oxygen breathing challenge. OXi8007 was administered IP *in situ* (350 mg/kg) and eighteen more pO_2 measurements were obtained over 2 hours followed by three to five measurements with air breathing.

MRI data were processed using Matlab (MathWorks Inc., Natick, MA) scripts. Tumor pO_2 was measured using *FREDOM* and R_1 (= 1/T_1) was estimated on a voxel-by-voxel basis using a monoexponential function:

$$SI = S_0 \left(1 - e^{-Tau/T_1}\right) + k \qquad [1]$$

where SI is signal intensity at recovery time Tau, S_0 represents the original magnetization and k is a constant. pO_2 (Torr) was determined using the calibration curve (reported at 37°C and 4.7 Tesla) [25]:

$$pO_2 = \frac{R_1 - 0.0835}{0.001876} \qquad [2]$$

Voxel-by-voxel measurements allowed calculation of $HF_{5, 10}$ (hypoxic fractions of voxels with pO_2 < 5 Torr and < 10 Torr, respectively). Only voxels with consistently reliable relaxation curve fitting (coefficient of determination, R^2 > 0.95) throughout the experiment were selected for further statistical analysis [27].

Results

Monitoring efficacy of OXi8007 with BLI

Bioluminescence images and time courses of three representative mice showed differential response to the VDAs (**Figure 2**). Maximum BLI signal occurred about 15 minutes after SC injection of luciferin. Of the 14 mice used for BLI, two (one saline control and one in the CA4P group) were only monitored for baseline, 4 and 24 hours. One mouse receiving CA4P died before the 72 hour time point; all the others were monitored for up to 72 hours and statistics are based on those tumors monitored for the full 72 hrs. Light emission tended to increase for the control tumors on the animals receiving saline on the five occasions over a period of 72 hours, with maximum total flux ranging from 1.6 × 10^7 to 4.3 × 10^8 p/s (mean
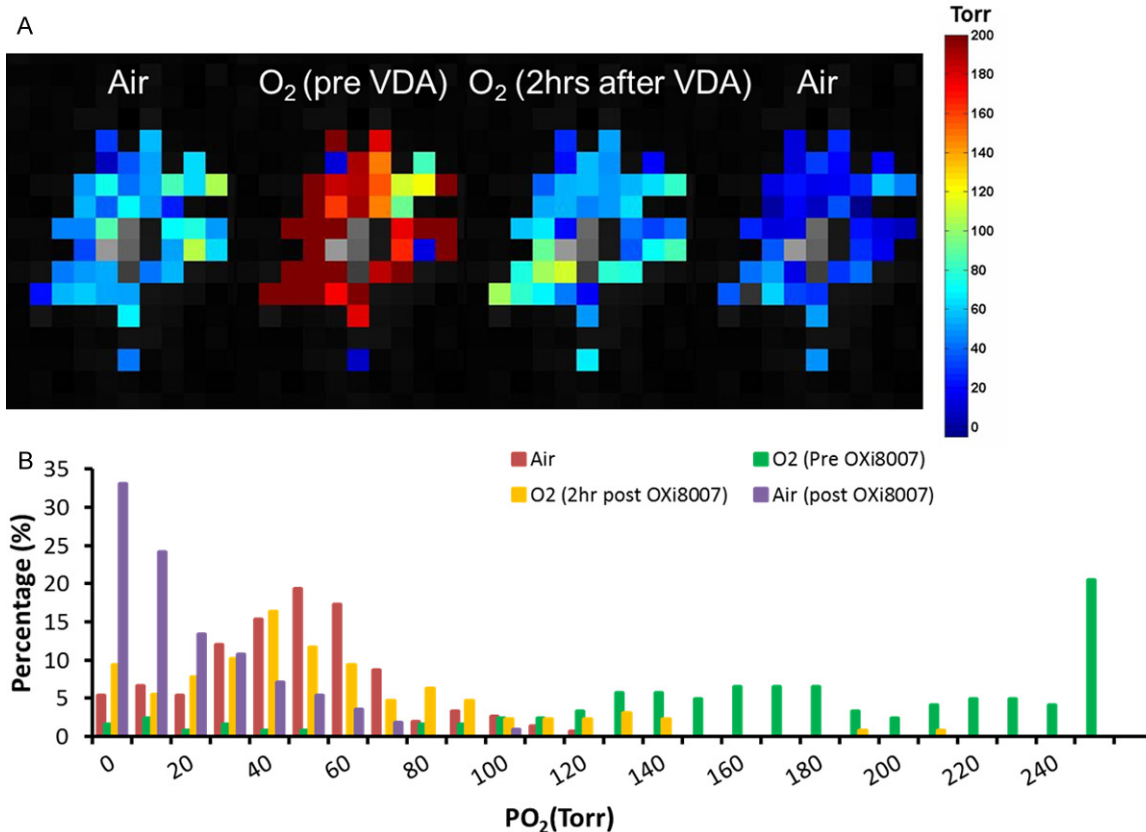
Figure 4. Dynamic pO_2 changes assessed using *FREDOM*. A. pO_2 maps of a representative tumor during baseline air breathing; 20 mins after switch to O_2-breathing; 2 hours after administration of OXi8007 (350 mg/kg), while continuing to breathe O_2 and after final switch back to air (left to right). B. Histogram showing pO_2 distributions at the four stages. Mean pO_2 and hypoxic fractions (HF_5 and HF_{10}) were respectively: baseline air-breathing (three dynamics), 47 Torr, 4%, 5%; baseline O_2-breathing (last three dynamics before VDA administration), 228 Torr, 0.7%, 0.7%; O_2-breathing two hours post OXi8007 administration (last five dynamics with stable pO_2 measurements before switching gas back to air), 58 Torr, 5%, 7%; air-breathing post OXi8007 (last three dynamics with stable pO_2 measurements), 12 Torr, 29%, 40%.

± SE = $1.5 \times 10^8 \pm 1.54 \times 10^8$ p/s; n = 4; mean baseline tumor volume = 544 ± 40 mm³). Following CA4P administration the maximum total BLI signal flux was significantly lower at all time points up to 48 hours. The lowest signal was observed at 4 hours (2.1×10^6 vs. 8.5×10^7 p/s baseline), representing a 97% average reduction, for the four tumors (mean baseline tumor volume = 569 ± 83 mm³). BLI signal remained low (less than 10% of baseline signal intensity) until 48 hours after injection, but recovered to 45% of original signal by 72 hours. For OXi8007, the signal decreased from mean baseline of 2.2×10^8 to 4.7×10^6 p/s at 4 hours (98% decline, n = 6; mean baseline tumor volume = 705 ± 50 mm³), and remained significantly depressed compared with baseline after 72 hrs. Up to 48 hrs both the CA4P and OXi8007 signals were significantly decreased compared with saline, but did not differ between agents.

At the 72 hour time point the integrated BLI (area under the curve) of OXi8007 remained significantly depressed compared with baseline (p < 0.0001). Data are summarized for the groups in **Figure 3**. Although tumor volumes of the cohorts at baseline were slightly different there was no significant difference based on two-way Student's t-test.

Changes of tumor pO_2 assessed by FREDOM

Dynamic pO_2 maps are shown for a representative tumor with respect to oxygen gas breathing challenge and administration of OXi8007 (**Figure 4**). Baseline pO_2 was measured in about 50 voxels simultaneously (**Figure 4A** shows the 40 common voxels which could be followed over 200 minutes) revealing heterogeneity in pO_2. The tumor was mostly well-oxygenated (mean pO_2 = 47 ± 25 Torr) with small hypoxic
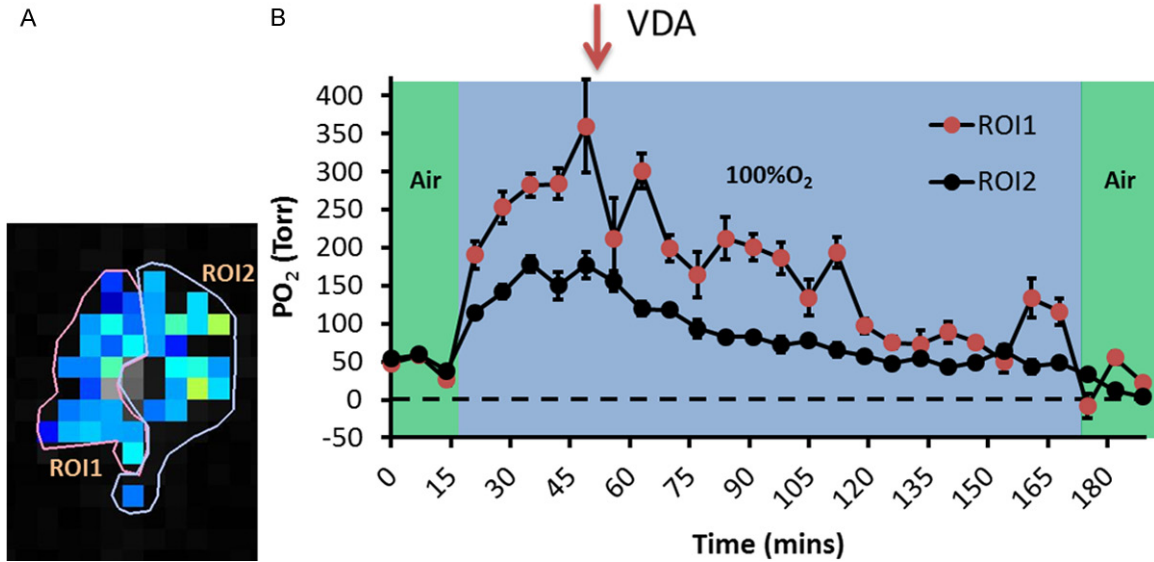
Figure 5. Intra-tumoral heterogeneity of response to O_2 breathing and OXi8007. A. Two ROIs were identified as more and less responsive in the tumor presented in **Figure 4**. B. Mean pO_2 of each region revealing differential dynamic response. Error bar representing standard error is used to demonstrate the spread of pixel pO_2 values within ROIs.
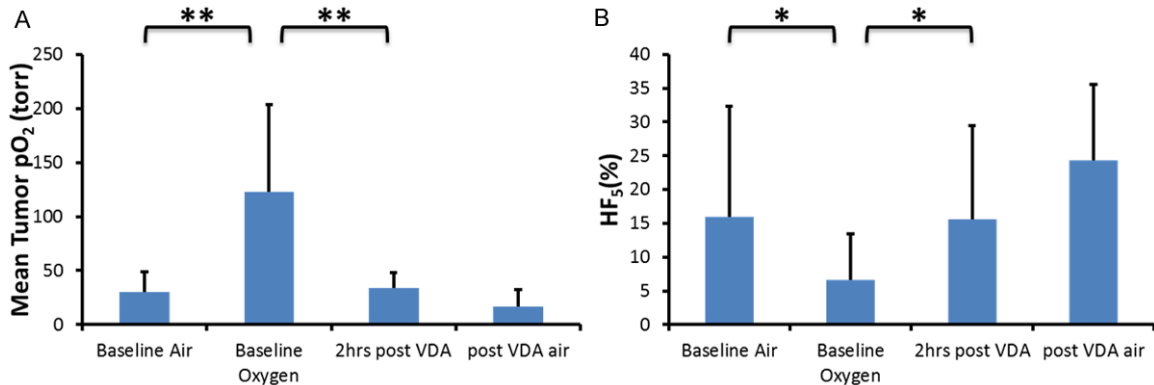

Figure 6. Tumor oxygenation with respect to intervention. Population mean and standard deviation of tumor pO_2 (A) and hypoxic fraction, HF_5 (B) in response to gas intervention and OXi8007. **indicating $p < 0.005$, *indicating $p < 0.05$.

fractions (HF_5 and HF_{10} = 4%, and = 5%, respectively; **Figure 4B**). Hypoxia was essentially eliminated with O_2-breathing and pO_2 increased significantly to mean pO_2= 228 ± 80 Torr ($p < 0.001$). Two hours post OXi8007 administration, pO_2 decreased approaching the baseline values (mean pO_2= 58 ± 40 Torr, HF_5 = 7%, HF_{10} = 9%) although the mouse continued to breathe oxygen. Upon switching to air-breathing, pO_2 declined further (mean pO_2 = 12 ± 22 Torr, HF_5 = 24%, HF_{10} = 33%). Baseline heterogeneity was apparent in individual tumor regions as well as differential response to oxygen breathing and OXi8007 (**Figure 5**).

Changes in mean pO_2 for the group of six mice are summarized in **Figure 6A**. Baseline pO_2, while breathing air was relatively stable for individual tumors (*e.g.*, **Figure 5B**) and ranged from a mean of 6 to 50 Torr with a population mean 31 ± 18 Torr (**Figure 6**). A significant increase accompanied oxygen breathing challenge (**Figure 6**; mean pO_2 = 123 ± 64 Torr, $p < 0.001$). Following administration of OXi8007, the pO_2 decreased significantly and stabilized around the baseline pO_2, although mice were still breathing oxygen (mean pO_2 = 34 ± 20 Torr). A further decrease in pO_2 was observed upon switching back to air breathing (mean pO_2 = 17

± 8 Torr). Meanwhile, hypoxic fraction (HF$_5$) was initially 16 ± 16% when the animals were breathing air, which decreased to 7 ± 6% when breathing oxygen (p < 0.05), rose to 16 ± 14% two hours after OXi8007 administration, and increased further to 24 ± 11% with final air breathing (**Figure 6B**).

Discussion

Serial BLI and *FREDOM* MRI were successfully applied to examine perfusion changes and hypoxiation induced by the novel VDA prodrug OXi8007 in orthotopic MDA-MB-231/luc human breast cancer xenografts in mice. BLI showed rapid vascular shut-down after administration of OXi8007 and the effect was greater and prolonged compared to a standard dose of the well-established VDA, CA4P. *FREDOM* revealed acute progressive hypoxiation in response to OXi8007. pO$_2$ maps indicated intra-tumor heterogeneity both with respect to oxygen breathing challenge and in response to OXi8007, though ultimately all tumor regions became hypoxic.

Many studies have demonstrated the rapid vascular shutdown caused by various VDAs in diverse tumor types including both human tumor xenografts in mice, as well as various other species [1, 8, 15-17]. Indeed, CA4P is subject to ongoing clinical trials [2, 28, 29]. However, the vascular effects were often found to be transient, *e.g.*, CA4P showed vascular disrupting effects followed by partial or full recovery as early as 24 hours both in clinical trials [28] and animal studies [30, 31]. Notably, a surviving ring of peripheral tumor is often observed [20, 30, 32, 33], which leads to rapid regrowth and little tumor growth delay following a single dose of CA4P [34]. CA4P has shown efficacy in combination with additional treatments such as irradiation and various chemotherapeutics [21, 32, 35, 36], but there is an active search for more effective agents, ideally demonstrating prolonged efficacy, while retaining selectivity and avoiding systemic toxicity. The synthesis of OXi8007 was recently described together with a preliminary indication of selective tumor vascular shutdown based on color-Doppler ultrasound over a period of 90 minutes [12]. The goal of the current study was to demonstrate efficacy in an alternate tumor type (here breast cancer as opposed to previous PC3 prostate cancer), explore longer term sequelae (up to 72 hours) and detail the consequences of induced ischemia in terms of induced hypoxia.

As reported previously, BLI generally provided a reproducible indication of tumor perfusion based on repeat measures [16, 17]. We have previously found that sequential measurements are usually consistent within about 20%, including in MDA-MB-231/luc tumors in mice [16]. In the past, we have sometimes observed a significant increase in BLI signal within 24 hours attributable to rapid tumor growth and increased volume generating greater signal, most notably in the fast growing MCF7 [16, 17]. Here we found very similar results at baseline and 4 hours, as well as 24 and 48 hours (**Figure 2**, control), but overall trend of increased signal for 5 measurements, as expected to accompany tumor growth. Many studies have shown that in the absence of therapy, the BLI intensity is proportional to tumor burden, although reaching a plateau for larger tumors [14, 16, 17, 37, 38].

As expected the control VDA, CA4P, caused extensive vascular shutdown within 4 hours. We previously reported 99% lower BLI signal in this tumor type at 4 hours after CA4P [15]. In this study we observed some recovery after 4 hours (2.6%) and return to 77% of baseline by 72 hours. The time to recovery appeared somewhat longer than we have observed previously in other tumors types (*e.g.*, MCF7) and using other modalities (*e.g.*, dynamic fluorescent imaging (DyCE) [31]).

The new experimental agent OXi8007 showed a very similar early response to CA4P with similar effectiveness at 4 hours (99% vs. 97%), though BLI signal was lower after 72 hours. The initial shutdown is in line with our previous preliminary observation using color-Doppler ultrasound in a PC3 prostate xenograft in a SCID mouse [17]. We have also examined a separate cohort of MDA-MB-231/luc tumors with respect to OXi8007 dose escalation over the acute 24 hrs timeframe and found very similar results (manuscript in preparation). We note that few investigations have reported long-term physiological effects of VDAs in tumors, generally reporting acute response over the first 2 to 4 hours or up to 24 hrs [1, 4, 18, 28, 29, 39, 40].

As expected vascular shutdown was accompanied by hypoxiation, with HF_{10} reaching 23% after 2 hours. This is in line with a previous study in a 13762NF syngeneic rat tumor growing in rats following CA4P administration, although in that case the hypoxia appeared more extensive [20]. VDAs are unlikely to be used as a mono-therapeutic agent, but rather in combination with other therapies [2, 18, 29, 41]. Thus, the time course of physiologic changes is important. Vascular shutdown would likely impair delivery of other chemotherapeutics, so that timing of administration is crucial [41]. Irradiation may be particularly appropriate since it targets the well vascularized and oxygenated regions most effectively; primarily the tumor periphery which appears to resist the action of VDAs [18, 42]. However, VDAs cause hypoxiation and thus could be expected to reduce the efficacy to irradiation, if inappropriate sequence or timing are applied. Therefore, the sequence and interval of treatment planning has shown strong influence towards efficacy when combining VDA with irradiation [42]. Many studies have shown VDAs induce hypoxia in the tumor, which is known to cause radiation resistance [43]. Horsman *et al.* measured pO_2 using Eppendorf electrodes and showed that pO_2 decreased significantly three hours after the administration of ZD6126 (a colchicine inspired experimental VDA) in a C3H mammary carcinoma mouse model [19]. Zhao *et al.* showed pO_2 decreased significantly within 90 minutes of CA4P injection using FREDOM in a 13762NF rat breast carcinoma model [20]. In our study, pO_2 decreased significantly from 122 ± 64 Torr (HF_5 = 7 ± 7%) to 34 ± 20 Torr (16 ± 14%) reaching a plateau 60-90 minutes after IP injection of OXi8007, while the animals were breathing oxygen. Evidence has been presented in human melanomas growing in nude mice that reduced bioluminescent light emission accompanying vascular disruption caused by the agent DMXAA was primarily attributable to hypoxiation [44]. We have not attempted to separate the effects of luciferin delivery versus hypoxiation here, but note that both are relevant. Oximetry was only performed for 2 hours following OXi8007 administration due to the relatively invasive procedure and fragility of mice under anesthesia. Generally, fresh hexafluorobenzene reporter molecule would be required at later time points, although we were able to evaluate pO_2 in rat tumors with respect to CA4P up to 24 hrs [20].

The MDA-MB-231 tumor is particularly popular in many investigations of breast cancer therapy, being triple-negative [45]. As such characterizing the extent of hypoxia pre therapy is itself important. It has often been assumed that tumors are hypoxic and therefore the small hypoxic fractions observed at baseline here, and ability to increase pO_2 with oxygen breathing may be important in using this model for studies of radiation response.

In presenting the dynamic BLI and *FREDOM* assessments here, it is important to note the many other approaches to assessing dynamic response to therapy, specifically in relation to vascular disruption [1]. Notably, rapid vascular shut-down in tumors after administration of CA4P to animals and patients has also been observed using radionuclides based on counting excised tissues following administration of ^{86}RbCl [46] or positron emission tomography (PET) of the distribution of ^{15}O water [47], Gd-DTPA dynamic contrast enhanced (DCE) MRI [15, 48, 49], DCE computed tomography (CT) of iobitridol [50], DCE fluorescent imaging of indocyanine green (DyCE) [31], ^{19}F MRI of tumor oxygenation using hexafluorobenzene [20], ^{1}H MRI of tumor oxygenation using hexamethyldisiloxane [24], Laser Doppler flowmetry [51], near infrared spectroscopy [21], interstitial fluid pressure (IFP) [51] and intra vital microscopy [8].

Advantages of dynamic BLI are high sensitivity, high throughput and cost efficiency. However, it indicates global perfusion changes of the tumor without revealing heterogeneity. BLI also requires cells transfected to express luciferase. *FREDOM* MRI revealed the spatial heterogeneity in response to VDA treatment and the onset of hypoxia. Other oximetry techniques could be applied such as electrodes, though they generally sample a single location only. Non-invasive imaging techniques usually require systemic delivery of a reporter molecule, and a recent study suggested that distribution of an agent such as nitroimidazole may be seriously perturbed by the ischemia, therefore failing to reflect hypoxia [39]. *FREDOM* using intratumoral injection of reporter molecule can provide absolute pO_2 measurements regardless of the perfusion changes, therefore providing lon-

gitudinal pO_2 assessment even in areas with limited blood access. It will be interesting to see whether new non-invasive approaches such as MRI-based Oxygen imaging (MOXI) [52] and mapping of oxygen by imaging lipids relaxation enhancement (MOBILE) [53] are able to provide reliable measurements of pO_2 in tumors with respect to VDAs in the future. We have successfully applied NIR non-invasively, but this reflected global vascular hypoxiation without providing spatial resolution [21].

Conclusion

In this study, we demonstrated the vascular disruption effect of the indole-based, small-molecule VDA referred to as OXi8007 both using BLI and *FREDOM* MRI. OXi8007 showed both a stronger and longer vascular disrupting effect than CA4P. *FREDOM* showed a significant decrease of pO_2 immediately after the administration of OXi8007. The response in the tumor is heterogeneous, but eventually a similar level of hypoxia was reached throughout the tumor.

Acknowledgements

Address correspondence to: Dr. Ralph P Mason, Department of Radiology, UT Southwestern Medical Center, 5323 Harry Hines Blvd. Dallas, TX 75390-9058, USA. Tel: +1-214-648-8926; Fax: +1-214-648-2991; E-mail: Ralph.Mason@UTSouthwestern.edu

References

[1]   Mason RP, Zhao D, Liu L, Trawick ML and Pinney KG. A perspective on vascular disrupting agents that interact with tubulin: preclinical tumor imaging and biological assessment. Integr Biol 2011; 3: 375-387.

[2]   Siemann DW. The unique characteristics of tumor vasculature and preclinical evidence for its selective disruption by Tumor-Vascular Disrupting Agents. Cancer Treat Rev 2011; 37: 63-74.

[3]   Thorpe PE. Vascular targeting agents as cancer therapeutics. Clin Cancer Res 2004; 10: 415-427.

[4]   Baish JW, Gazit Y, Berk DA, Nozue M, Baxter LT and Jain RK. Role of Tumor Vascular Architecture in Nutrient and Drug Delivery: An Invasion Percolation-Based Network Model. Microvasc Res 1996; 51: 327-346.

[5]   Kerbel RS. A cancer therapy resistant to resistance. Nature 1997; 390: 335-336.

[6]   Blakey DC, Ashton SE, Westwood FR, Walker M and Ryan AJ. ZD6126: A novel small molecule vascular targeting agent. Int J Radiat Oncol Biol Phys 2002; 54: 1497-1502.

[7]   Tozer GM, Kanthou C and Baguley BC. Disrupting tumour blood vessels. Nat Rev Cancer 2005; 5: 423-435.

[8]   Tozer GM, Prise VE, Wilson J, Cemazar M, Shan SQ, Dewhirst MW, Barber PR, Vojnovic B and Chaplin DJ. Mechanisms associated with tumor vascular shut-down induced by combretastatin A-4 phosphate: Intravital microscopy and measurement of vascular permeability. Cancer Res 2001; 61: 6413-6422.

[9]   Brown JM and Giaccia AJ. The Unique Physiology of Solid Tumors: Opportunities (and Problems) for Cancer Therapy. Cancer Res 1998; 58: 1408-1416.

[10]   Bhattacharyya B, Panda D, Gupta S and Banerjee M. Anti-mitotic activity of colchicine and the structural basis for its interaction with tubulin. Med Res Rev 2008; 28: 155-183.

[11]   Pinney KG, Pettit GR, Trawick ML, Jelinek C and Chaplin DJ. Antitumor Agents from Natural Products. Boca Raton, FL: CRC Press, Taylor and Francis Group, 2011.

[12]   Hadimani MB, MacDonough MT, Ghatak A, Strecker TE, Lopez R, Sriram M, Nguyen BL, Hall JJ, Kessler RJ, Shirali AR, Liu L, Garner CM, Pettit GR, Hamel E, Chaplin DJ, Mason RP, Trawick ML and Pinney KG. Synthesis of a 2-Aryl-3-aroyl Indole Salt (OXi8007) Resembling Combretastatin A-4 with Application as a Vascular Disrupting Agent. J Nat Prod 2013; 76: 1668-1678.

[13]   Pinney KG, Wang F, Hadimani M and Mejia MDP. Indole-containing compounds with anti-tubulin and vascular targeting activity. United States patent (2007) #20070082872.

[14]   Contag CH and Ross BD. It's not just about anatomy: In vivo bioluminescence imaging as an eyepiece into biology. J Magn Reson Im 2002; 16: 378-387.

[15]   Zhao D, Richer E, Antich PP and Mason RP. Antivascular effects of combretastatin A4 phosphate in breast cancer xenograft assessed using dynamic bioluminescence imaging and confirmed by MRI. FASEB J 2008; 22: 2445-2451.

[16] Liu L, Beck H, Wang X, Hsieh HP, Mason RP and Liu X. Tubulin-Destabilizing Agent BPROL075 Induces Vascular-Disruption in Human Breast Cancer Mammary Fat Pad Xenografts. PLoS One 2012; 7: e43314.

[17] Alhasan MK, Liu L, Lewis MA, Magnusson J and Mason RP. Comparison of Optical and Power Doppler Ultrasound Imaging for Non-Invasive Evaluation of Arsenic Trioxide as a Vascular Disrupting Agent in Tumors. PLoS One 2012; 7: e46106.

[18] Horsman MR and Siemann DW. Pathophysiologic Effects of Vascular-Targeting Agents and the Implications for Combination with Conventional Therapies. Cancer Res 2006; 66: 11520-11539.

[19] Horsman MR, Ehrnrooth E, Ladekarl M and Overgaard J. The effect of combretastatin A-4 disodium phosphate in a C3H mouse mammary carcinoma and a variety of murine spontaneous tumors. Int J Radiat Oncol Biol Phys 1998; 42: 895-898.

[20] Zhao D, Jiang L, Hahn EW and Mason RP. Tumor physiologic response to combretastatin A4 phosphate assessed by MRI. Int J Radiat Oncol Biol Phys 2005; 62: 872-880.

[21] Zhao D, Chang CH, Kim JG, Liu H and Mason RP. In Vivo Near-Infrared Spectroscopy and Magnetic Resonance Imaging Monitoring of Tumor Response to Combretastatin A-4-Phosphate Correlated With Therapeutic Outcome. Int J Radiat Oncol Biol Phys 2011; 80: 574-581.

[22] Brown JM. The Hypoxic Cell: A Target for Selective Cancer Therapy-Eighteenth Bruce F. Cain Memorial Award Lecture. Cancer Res 1999; 59: 5863-5870.

[23] Krohn KA, Link JM and Mason RP. Molecular Imaging of Hypoxia. J Nucl Med 2008; 49: 129S-148S.

[24] Mason RP, Zhao D, Pacheco-Torres J, Cui W, Kodibagkar VD, Gulaka PK, Hao G, Thorpe P, Hahn EW and Peschke P. Multimodality imaging of hypoxia in preclinical settings. Q J Nucl Med Mol Imaging 2010; 25: 259-280.

[25] Zhao D, Jiang L and P. Mason R. Measuring Changes in Tumor Oxygenation. Methods in Enzymology 2004; 386: 378-418.

[26] Vilalta M, Rafat M, Giaccia Amato J and Graves Edward E. Recruitment of Circulating Breast Cancer Cells Is Stimulated by Radiotherapy. Cell Rep 2014; 8: 402-409.

[27] Hallac RR, Zhou H, Pidikiti R, Song K, Stojadinovic S, Zhao D, Solberg T, Peschke P and Mason RP. Correlations of noninvasive BOLD and TOLD MRI with pO2 and relevance to tumor radiation response. Magn Reson Med 2014; 71: 1863-1873.

[28] Galbraith SM, Maxwell RJ, Lodge MA, Tozer GM, Wilson J, Taylor NJ, Stirling JJ, Sena L, Padhani AR and Rustin GJS. Combretastatin A4 Phosphate Has Tumor Antivascular Activity in Rat and Man as Demonstrated by Dynamic Magnetic Resonance Imaging. J Clin Oncol 2003; 21: 2831-2842.

[29] Siemann DW, Chaplin DJ and Walicke PA. A review and update of the current status of the vasculature-disabling agent combretastatin-A4 phosphate (CA4P). Expert Opin Invest Drugs 2009; 18: 189-197.

[30] Prise VE, Honess DJ, Stratford MRL, Wilson J and Tozer GM. The vascular response of tumor and normal tissues in the rat to the vascular targeting agent, combretastatin A-4-phosphate, at clinically relevant doses. Int J Oncol 2002; 21: 717-726.

[31] Liu L, Su X and Mason RP. Dynamic Contrast Enhanced Fluorescent Molecular Imaging of Vascular Disruption Induced by Combretastatin-A4P in Tumor Xenografts. J Biomed Nanotechnol 2014; 10: 1545-1551.

[32] Grosios K, Loadman PM, Swaine DJ, Pettit GR and Bibby MC. Combination chemotherapy with combretastatin A-4 phosphate and 5-fluorouracil in an experimental murine colon adenocarcinoma. Anticancer Res 2000; 20: 229-233.

[33] Salmon BA and Siemann DW. Characterizing the Tumor Response to Treatment With Combretastatin A4 Phosphate. Int J Radiat Oncol Biol Phys 2007; 68: 211-217.

[34] Chaplin DJ, Pettit GR and Hill SA. Anti-vascular approaches to solid tumour therapy: evaluation of combretastatin A4 phosphate. Anticancer Res 1999; 19: 189-195.

[35] Nathan P, Zweifel M, Padhani AR, Koh DM, Ng M, Collins DJ, Harris A, Carden C, Smythe J, Fisher N, Taylor NJ, Stirling JJ, Lu SP, Leach MO, Rustin GJS and Judson I. Phase I Trial of Combretastatin A4 Phosphate (CA4P) in Combination with Bevacizumab in Patients with Advanced Cancer. Clin Cancer Res 2012; 18: 3428-3439.

[36] Griggs J, Metcalfe JC and Hesketh R. Targeting tumour vasculature: the development of combretastatin A4. Lancet Oncol 2001; 2: 82-87.

[37] O'Neill K, Lyons SK, Gallagher WM, Curran KM and Byrne AT. Bioluminescent imaging: a critical tool in pre-clinical oncology research. J Pathol 2009; 220: 317-327.

[38] Paroo Z, Bollinger RA, Braasch DA, Richer E, Corey DR, Antich PP and Mason RP. Validating Bioluminescence Imaging as a High-Throughput, Quantitative Modality for Assessing Tumor Burden. Mol Imaging 2004; 3: 117-24.

[39] Oehler C, O'Donoghue JA, Russell J, Zanzonico P, Lorenzen S, Ling CC and Carlin S. 18F-Fluromisonidazole PET Imaging as a Biomarker for the Response to 5,6-Dimethylxanthenone-4-Acetic Acid in Colorectal Xenograft Tumors. J Nucl Med 2011; 52: 437-444.

[40] Diepart C, Karroum O, Magat J, Feron O, Verrax J, Calderon PB, Gregoire V, Leveque P, Stockis J, Dauguet N, Jordan BF and Gallez B. Arsenic Trioxide Treatment Decreases the Oxygen Consumption Rate of Tumor Cells and Radiosensitizes Solid Tumors. Cancer Res 2012; 72: 482-490.

[41] Siemann DW, Mercer E, Lepler S and Rojiani AM. Vascular targeting agents enhance chemotherapeutic agent activities in solid tumor therapy. Int J Cancer 2002; 99: 1-6.

[42] Murata R, Siemann DW, Overgaard J and Horsman MR. Interaction between combretastatin A-4 disodium phosphate and radiation in murine tumors. Radiother Oncol 2001; 60: 155-161.

[43] Gray LH, Conger AD, Ebert M, Hornsey S and Scott OCA. The Concentration of Oxygen Dissolved in Tissues at the Time of Irradiation as a Factor in Radiotherapy. Br J Radiol 1953; 26: 638-648.

[44] Cecic I, Chan DA, Sutphin PD, Ray P, Gambhir SS, Giaccia AJ and Graves EE. Oxygen sensitivity of reporter genes: Implications for preclinical imaging of tumor hypoxia. Mol Imaging 2007; 6: 219-228.

[45] Lehmann BD, Bauer JA, Chen X, Sanders ME, Chakravarthy AB, Shyr Y and Pietenpol JA. Identification of human triple-negative breast cancer subtypes and preclinical models for selection of targeted therapies. J Clin Invest 2011; 121: 2750-2767.

[46] Eikesdal HP, Bjerkvig R, Mella O and Dahl O. Combretastatin A-4 and hyperthermia;a potent combination for the treatment of solid tumors. Radiother Oncol 2001; 60: 147-154.

[47] Anderson HL, Yap JT, Miller MP, Robbins A, Jones T and Price PM. Assessment of pharmacodynamic vascular response in a phase I trial of combretastatin A4 phosphate. J Clin Oncol 2003; 21: 2823-2830.

[48] Maxwell RJ, Wilson J, Prise VE, Vojnovic B, Rustin GJ, Lodge MA and Tozer GM. Evaluation of the anti-vascular effects of combretastatin in rodent tumours by dynamic contrast enhanced MRI. NMR Biomed 2002; 15: 89-98.

[49] Beauregard DA, Pedley RB, Hill SA and Brindle KM. Differential sensitivity of two adenocarcinoma xenografts to the anti-vascular drugs combretastatin A4 phosphate and 5,6-dimethylxanthenone-4-acetic acid, assessed using MRI and MRS. NMR Biomed 2002; 15: 99-105.

[50] Ng QS, Goh V, Carnell D, Meer K, Padhani AR, Saunders MI and Hoskin PJ. Tumor Antivascular Effects of Radiotherapy Combined with Combretastatin A4 Phosphate in Human Non-Small-Cell Lung Cancer. Int J Radiat Oncol Biol Phys 2007; 67: 1375-1380.

[51] Ley CD, Horsman MR and Kristjansen PEG. Early effects of combretastatin-A4 disodium phosphate on tumor perfusion and interstitial fluid pressure. Neoplasia 2007; 9: 108-112.

[52] Zhang Z, Hallac RR, Peschke P and Mason RP. A noninvasive tumor oxygenation imaging strategy using magnetic resonance imaging of endogenous blood and tissue water. Magn Reson Med 2014; 71: 561-569.

[53] Jordan BF, Magat J, Colliez F, Ozel E, Fruytier AC, Marchand V, Mignion L, Bouzin C, Cani PD, Vandeputte C, Feron O, Delzenne N, Himmelreich U, Denolin V, Duprez T and Gallez B. Mapping of oxygen by imaging lipids relaxation enhancement: A potential sensitive endogenous MRI contrast to map variations in tissue oxygenation. Magn Reson Med 2013; 70: 732-744.